



Original Research Article

Aromatization of LPG over ZnO/ZSM-5 Catalysts: Statistical Optimization of Process Variables

¹Isa, A.R., ¹Gbadamasi, S., ¹Fasanya, O.O., ¹Ahmed, U.O., ¹Gano, Z.S., ^{*2}Atta, A.Y.,
²Mukhtar, B., ²Aderemi, B.O. and ²Jibril, B.Y.

¹Petrochemicals Department, National Research Institute for Chemical Technology, Zaria, Nigeria.

²Department of Chemical Engineering, Ahmadu Bello University, Zaria, Nigeria.

*zeezoatta@gmail.com

ARTICLE INFORMATION

Article history:

Received 04 May, 2019

Revised 26 May, 2019

Accepted 28 May, 2019

Available online 30 June, 2019

Keywords:

LPG

Aromatization

Aromatics

ZnO

ZSM-5

RSM

ABSTRACT

Research efforts are being made regarding one-step production of petrochemical feedstocks from natural gas, liquefied petroleum gas (LPG) and natural gas liquids (NGLs) which will guarantee the continuous supply of hydrocarbon chemical feedstocks. In this regard, a statistical approach for optimizing the process variables (reaction temperature, catalyst weight and zinc oxide (ZnO) wt% loading on ZSM-5) in LPG aromatization over ZnO/ZSM-5 catalyst was carried out in this work. Three different ZnO loaded ZSM-5 (Si/Al=50) catalysts were prepared and characterized by N₂ adsorption-desorption, XRD, UV-Vis, SEM, and IR spectra of pyridine adsorption. D-optima experimental design was used to establish the interaction effects of the variables towards LPG conversion and aromatic selectivity while response surface methodology (RSM) was employed in optimizing the experimental process variables in the aromatization process. A second order regression model was developed and the coefficient of determination (R²) was determined to be 95.61%. Optimum LPG conversion of 94.75% was achieved at 520 °C for 0.245 g catalyst weight and 5 wt% ZnO loading with a corresponding aromatic selectivity of 22.38%.

© 2019 RJEES. All rights reserved.

1. INTRODUCTION

The availability of transportation fuel and petrochemical feedstock is threatened due to dwindling global oil reserves and the predicament of oil price volatility together with stricter environmental regulations (Chen et al., 2015). These factors have heightened the search for cleaner and cheaper alternative energy sources and chemical feedstock (Majhi et al., 2013; Song et al., 2014; Chen et al., 2015). However, some possible alternative energy sources that can guarantee the continuous supply of these fuels and chemicals are natural gas, liquefied petroleum gas (LPG), natural gas liquids (NGLs) (Vosmerikova et al., 2014a; Chen et al., 2015). LPG is mostly composed of C₂-C₅ straight chain hydrocarbons and these hydrocarbons are also found

in natural gas as well as in NGLs (Matsuoka et al., 2000). Interestingly, these attractive sources can be converted using a one-stop catalyst that combines several steps to benzene, toluene, ethylbenzene and xylenes (BTEX); the three most important intermediates for the production of plastic, fibres, resins, dyestuffs, detergents and many other things of daily requirements (Al-Khattaf et al., 2014). Also, their conversion into these useful chemicals would increase the source of hydrocarbon products (Kitagawa et al., 1986).

Recent developments in zeolite processes have dramatically increased the demand for aromatic hydrocarbons (Vosmerikova et al., 2014b). To meet this demand, aromatization of light hydrocarbons, the components found in NG, LPG and NGLs, over zeolite catalysts have evolved. Various commercial processes such as cyclar from British Petroleum, aroforming from Salutec, z-forming from Mitsubishi and Chiyoda, have been established for LPG transformation into BTEX hydrocarbons with simultaneous formation of a large amount of hydrogen which is also a valuable product (Caeiro et al., 2006). A lot of interest has been paid to gallium or zinc-based ZSM-5 catalysts because of the improved aromatic hydrocarbon selectivity that was observed (Frey et al., 2011; Niu et al., 2014) As a result of their high dehydrogenating abilities, the presence of these metal ions (gallium and zinc) in the ZSM-5 catalyst helps in the hydrogen recombination and desorption with consequent improvement in the BTEX selectivity (Viswanadham et al., 2004).

A number of studies highlighted the role of zinc in the transformation of light hydrocarbons to aromatics. Mole *et al.* (1985) studied the role of zinc in propane activation and described it as a hydride acceptor in the formation of propyl carbenium ion (Mole et al., 1985). Report of Kitagawa *et al.* (1986) agreed with studies of Viswanadham *et al.* (2004) on the transformation of *n*-hexane to benzene by zinc and the acid sites present on ZSM-5 (Mole et al., 1985; Viswanadham et al., 2004). These affirmed the bifunctional mechanism being proposed that both zinc and ZSM-5 participate in the activation process (Ogunronbi et al., 2015). Also, Viswanadham *et al.* (2004) explained that zinc presence creates alternative routes for aromatization and inhibits the continuous oligomerization and formation of higher aromatics (Viswanadham et al., 2004). In all these studies, it has been found that experimental variables such as contact time, reactant partial pressures, reaction temperature, metal loading, catalyst weight, etc. influence the level of the conversion of the feedstock and the selectivity towards aromatics. Therefore, investigating the influence of these variables one-at-a-time becomes laborious and protracted. More so, this approach would be unable to determine the interaction effects amongst them. Consequently, these drawbacks motivated the adoption of response surface methodology (RSM) in the present study.

RSM is a statistical tool that is being employed to optimize any process where a number of independent variables affect the output of the desired product. This method easily allows for the study of interactions between two or more experimental process variables unlike the conventional approach, where one variable is studied while keeping the others constant, thereby making it impossible for the overall effects of all the variables to be studied at a time (Montgomery and Runger 2011). A number of studies have shown that RSM could be used as an effective optimization tool in experimental process. Majhi *et al.* (2013) employed RSM central composite design in optimizing methane conversion over Zn-Mo/H-ZSM-5 catalyst in the presence of methanol. They reported a second order regression model for the methane conversion and obtained 0.96 coefficient of determination (Majhi et al., 2013). Similarly, optimization of operational parameters for adsorption of heavy metals from industrial effluent on nano-adsorbents has been reported using the Box–Behnken design matrix. Dubey *et al.* (2016) demonstrated the use of RSM Box-Behnken design in determining the effects of process variables in the high uptake of Cr(VI) on the nano-particles (Dubey et al., 2016).

In this work, we report on the optimization studies of LPG aromatization process over ZnO supported ZSM-5 using RSM. RSM D-optimal becomes a design of choice because of its relatively high accuracy level with fewer experimental runs than Box-Behnken or central composite and much fewer than full factorial design.

This study was performed at different reaction temperatures (520 °C to 580 °C), varying catalyst:diluent ratios (0.0-0.5 g), and constant flowrates of LPG and nitrogen (20 ml/min and 80 ml/min respectively). Three catalysts with different zinc loadings were prepared via the impregnation method with ZSM-5 ($\text{SiO}_2/\text{Al}_2\text{O}_3=50$) as support. As-prepared catalysts were characterized and their performances investigated in a fixed bed reactor.

2. MATERIALS AND METHODS

2.1. Catalysts Preparation

Three catalysts containing 0.5, 2 and 5wt% zinc oxide, supported on ZSM-5 (Zeolyst) with a silica alumina ratio of 50 were prepared via the incipient wet impregnation method with an aqueous solution of $\text{Zn}(\text{NO}_3)_2 \cdot 6\text{H}_2\text{O}$ (BDH). The solutions were continuously stirred and kept at 80 °C to slowly evaporate the mixtures to dryness. The powders were further dried in an oven at 100 °C for 14 h. The final dried samples were calcined under air at 550 °C for 6 h.

2.2. Catalysts Characterization

The calcined samples were characterized by UV-Vis spectroscopy, pyridine IR, SEM, and X-ray diffractometry (XRD). The UV-Vis was used to determine the nature of ZnO deposition on the ZSM-5. Spectra of UV-Vis were obtained on a Shimadzu UV-2500PC Series spectrophotometer, using methanol as reference. The pyridine IR technique was employed in identifying the nature of acidic sites present on the catalyst samples. The IR measurements were conducted on a Shimadzu FTIR-8400S, Fourier Transform Infrared Spectrometer using ATR, in the range of 1400 cm^{-1} – 1700 cm^{-1} . The catalysts were first pretreated at 250 °C for 2 h under vacuum to remove any dissolved gases, and subsequently, pyridine vapor was flowed through for 1 h. Finally, the IR spectra were recorded on the Shimadzu FTIR-8400S using ATR. Structure and crystallinity of the calcined samples were obtained using an XRD PANalytical EMPYREAN diffractometer equipped with $\text{Cu-K}\alpha$ ($\lambda = 1.5406\text{ \AA}$) radiation source operating at 40 mA and 40 kV in the 2θ range of 5° to 60°. The scan step size was $0.013^\circ\text{ s}^{-1}$ and the ZnO crystallite size was calculated using the Scherrer equation from the diffraction peak at $d(100)$. Nitrogen sorption isotherms were performed at liquid nitrogen temperature (-196°C) on a GoldApp V-Sorp2800P surface area analyzer to determine the specific surface areas for the three catalysts. Prior to the sorption measurements, about 200 mg of each of the prepared catalyst was degassed at 200 °C until constant pressure was achieved.

2.3. Experimental Design

Statistical experimental design was done using three independent experimental process variables: reaction temperature, catalyst weight, and ZnO wt% loading on ZSM-5 (50). Reaction temperature and catalyst weight were grouped as numeric factors with range between 520°C to 580°C and 0.0-0.5g respectively. ZnO wt% loading on ZSM-5 was taken as a categoric factor with 3 levels depicting the 0.5, 2 and 5 wt% ZnO loading respectively. These ranges and levels of the factors were designated using D-Optima and are presented in Table 1. The design obtained was used in the study of LPG aromatization over ZnO/ZSM-5 catalysts. The aromatization process was optimized through three sequential stages: (i) statistical design of experiment (DOE), (ii) determination of coefficients in the mathematical model and prediction of the response, and (iii) testing the adequacy of the model. The responses (conversion and selectivity) obtained after experimentation were analyzed using ANOVA and coefficient of determination (R^2).

Table 1: D-Optima experimental design summary

Variables	Symbol	Type	Low (actual)	High (actual)
Reaction temperature (°C)	A	Numeric	520	580
Catalyst weight (g)	B	Numeric	0	0.5
Zn (wt%) loading	C	Categoric	0.5	5

2.4. Catalyst Testing

The activities of the prepared catalysts were tested in a continuous flow vertical fixed bed reactor with 11 mm internal diameter and 55 cm in length as per the design of experiment (DOE) (Table 2). In a typical run, 1 g of catalyst diluted with glass beads was charged into the reactor and supported at the centre with the aid of glass wool. A k-type thermocouple equipped with a PID controller was inserted into the catalyst bed to measure the temperature of the bed. Reactant streams consisted of LPG and Nitrogen at 20 ml/min and 80 ml/min respectively and regulated by calibrated mass flow controllers. Reactor exit stream was conducted by a line maintained at 150 °C and the analyses of the reaction mixtures were made by periodic sampling at 1 h intervals. Reaction products distribution were analyzed on-line with a gas chromatography (BUCK Scientific, model 910) equipped with a thermal conductivity detector (TCD) connected to both molesieve 13X and Hayesep D columns, and a flame ionization detector (FID) connected to a 60 m × 0.53 mm × 5 μm RestekMXT-1 capillary column. Peak areas were converted into mole percent by means of response factors determined through calibrations. LPG conversions (% X_{iC_4}) and BTEX selectivity (% S_{BTEX}) were defined as expressed in Equations (1) and (2) respectively:

$$X_{iC_4}(\%) = \frac{\text{Mole of } iC_4 \text{ in feed} - \text{Mole of } iC_4 \text{ in product}}{\text{Mole of } iC_4 \text{ in feed}} \times 100 \quad (1)$$

$$S_{BTEX}(\%) = \frac{\text{Mole of BTEX}}{\text{Mole of } iC_4 \text{ in feed} - \text{Mole of } iC_4 \text{ in product}} \times 100 \quad (2)$$

Table 2: RSM D-Optima design of experiment (DOE)

Run	Reaction temperature (°C)	Catalyst weight (g)	ZnO loading (wt%)
1	557.50	0.19	5
2	573.09	0.31	0.5
3	539.57	0.50	0.5
4	557.50	0.19	5
5	520.00	0.00	2
6	520.00	0.00	0.5
7	580.00	0.00	0.5
8	580.00	0.50	2
9	580.00	0.50	5
10	580.00	0.00	2
11	520.00	0.28	0.5
12	580.00	0.50	5
13	520.00	0.00	5
14	542.18	0.31	2
15	520.00	0.00	5
16	520.00	0.50	2
17	520.00	0.31	2
18	550.00	0.02	0.5
19	580.00	0.50	0.5
20	580.00	0.50	0.5
21	520.00	0.50	5
22	580.00	0.00	5
23	520.00	0.31	2
24	542.80	0.00	2

3. RESULTS AND DISCUSSION

3.1. Catalysts Characterization

Figure 1 shows the XRD patterns for the support (ZSM-5 (50)) and the corresponding catalysts (0.5-5 wt% ZnO loadings). The results show that the crystalline nature of the ZSM-5(50) was maintained upon calcination. The patterns for 0.5, 2, and 5 wt% ZnO loadings showed similar diffraction peaks as the parent ZSM-5 (50), except for slight increment of the peaks at $2\theta = 31.1^\circ$, 34.3° , and 36° . These peaks corresponded to the (100), (002), and (101) hexagonal structure of ZnO respectively (JCPDS 01-079-0208). The ZnO crystallite sizes of the catalysts, calculated by Scherrer equation using the peak d(100), are presented in Table 3. The results revealed that the average crystallite size of ZnO in each catalyst is larger than the corresponding pore diameter of the ZSM-5 (50) support. This observation suggests that some particles of the active component are deposited on the external surface of the support during impregnation which resulted in a decrease in the mesopore area.

The textural properties of ZSM-5 (50) and the corresponding ZnO loaded catalysts were investigated using N_2 adsorption-desorption analysis and the results are summarized in Table 3. The results obtained shows that support has a BET surface area of $358.7 \text{ m}^2/\text{g}$, an average pore volume of $0.1919 \text{ cm}^3/\text{g}$ and an average pore size of 34 \AA . In addition, the microporous section contributed an area of $225.1 \text{ m}^2/\text{g}$ to the BET surface area, which is almost twice the mesopore area of $133.6 \text{ m}^2/\text{g}$. However, there was a noticeable decrease in the BET surface area of the catalysts as ZnO was impregnated. ZnO impregnation resulted into possible surface coverage of the mesoporous section of the catalysts as evident from Table 3 and the decrease in surface area increases with increase in ZnO loading. Furthermore, there was also decrease in the average pore volume and average pore size of the catalysts upon impregnation. Expectedly, this decrease increases with increase in the ZnO loading and could be associated to partial pore blockage by the impregnated ZnO. Though there was a decrease in the average pore size, however, the final pore size still falls within the mesoporous region as per IUPAC classification (Condon 2006). This is a desirable property as it would enhance diffusivity during the aromatization reaction.

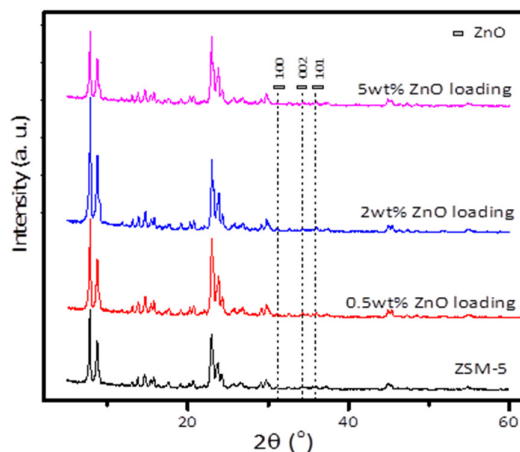


Figure 1: XRD patterns ZSM-5 (Si/Al=50) and the different ZnO wt% loadings on ZSM-5

Table 3: BET surface area measurements of the synthesized catalysts

Catalyst	BET (m ² /g)	Micropore area (m ² /g)	Mesopore area (m ² /g)	Average pore volume ^a (cm ³ /g)	Average pore size ^b (Å)	ZnO crystallite size ^c (Å)
ZSM-5 (50)	358.7	225.1	133.6	0.1919	34	–
0.5wt% ZnO	360.6	244.3	116.3	0.1750	29	460
2wt% ZnO	339.7	248.7	91.0	0.1615	29	537
5wt% ZnO	299.6	227.8	71.8	0.1429	26	403

^aBJH adsorption average pore diameter. ^bBJH adsorption pore volume. ^cCalculated by using Scherrer equation based on XRD results.

Figure 2 shows the SEM images and the corresponding EDX of the support, ZSM-5 (50) and the catalysts; 0.5, 2 and 5 wt% ZnO loadings. The images revealed highly crystalline ZSM-5(50) with hexagonal morphology. Upon impregnating ZnO, there was no observable change in the morphology of the parent ZSM-5(50), as the hexagonal structure was maintained. Though, the presence of ZnO could not be clearly seen from the SEM images, however, the EDX results confirmed its presence. In addition, ZnO could not be detected in the catalyst with 0.5 wt% ZnO loading, and this could be associated with the concentration of the zinc in the catalyst which might be below the detection limit of the machine used.

Pyridine, a weak base that can be titrated with strong acid sites, has the potential of neutralizing both Lewis and Bronsted acid sites in solid catalysts. Figure 3 shows the pyridine IR spectra for the parent ZSM-5(50) and the synthesized catalysts (5, 2 and 0.5wt% ZnO loading on ZSM-5(50)). The bands at 1443 and 1620 cm⁻¹ and at 1550 and 1647 cm⁻¹ are assigned to the presence of Lewis and Bronsted acid sites respectively. The band at 1490 cm⁻¹ is associated to the presence of both Bronsted and Lewis sites (Fripat et al., 1997; Gómez-Cazalilla et al., 2007; Dragoi et al., 2009). A phenomenon that is common to all the catalysts is the shift of peaks from 1443 to 1450 cm⁻¹, and from 1550 to 1544 cm⁻¹ as observed in the spectra. This phenomenon is associated to the external deposition of ZnO on the surface of the support (ZSM-5(50)) (Fripat et al., 1997; Dragoi et al., 2009). Furthermore, Ai *et al.* (2013) asserted that the presence of acidity in aromatization catalysts greatly influences the cracking and isomerization steps of the reaction, and as a result, improve the conversion (Ai et al., 2013). As seen from this pyridine analysis, all the synthesized catalysts have an increase in the intensity of their absorbance peaks, indicating an increase in acidity caused by the deposition of ZnO, consequently increasing LPG conversion potential.

Figure 4 shows the UV-Vis spectra of the catalysts, with ZSM-5 (50) as the reference point. Catalysts with 2 and 5wt% loadings show the presence of a peak at about 360 nm, which is due to the presence of ZnO nanoparticle (Premanathan et al., 2011; Goh et al., 2014). On the other hand, there was no noticeable peak on the catalyst with 0.5 wt% ZnO loading and it was identical to the parent ZSM-5 (50). The absence of peak on this catalyst is attributed to its low quantity of ZnO loading and the low detection limit of the UV-Vis analyzer.

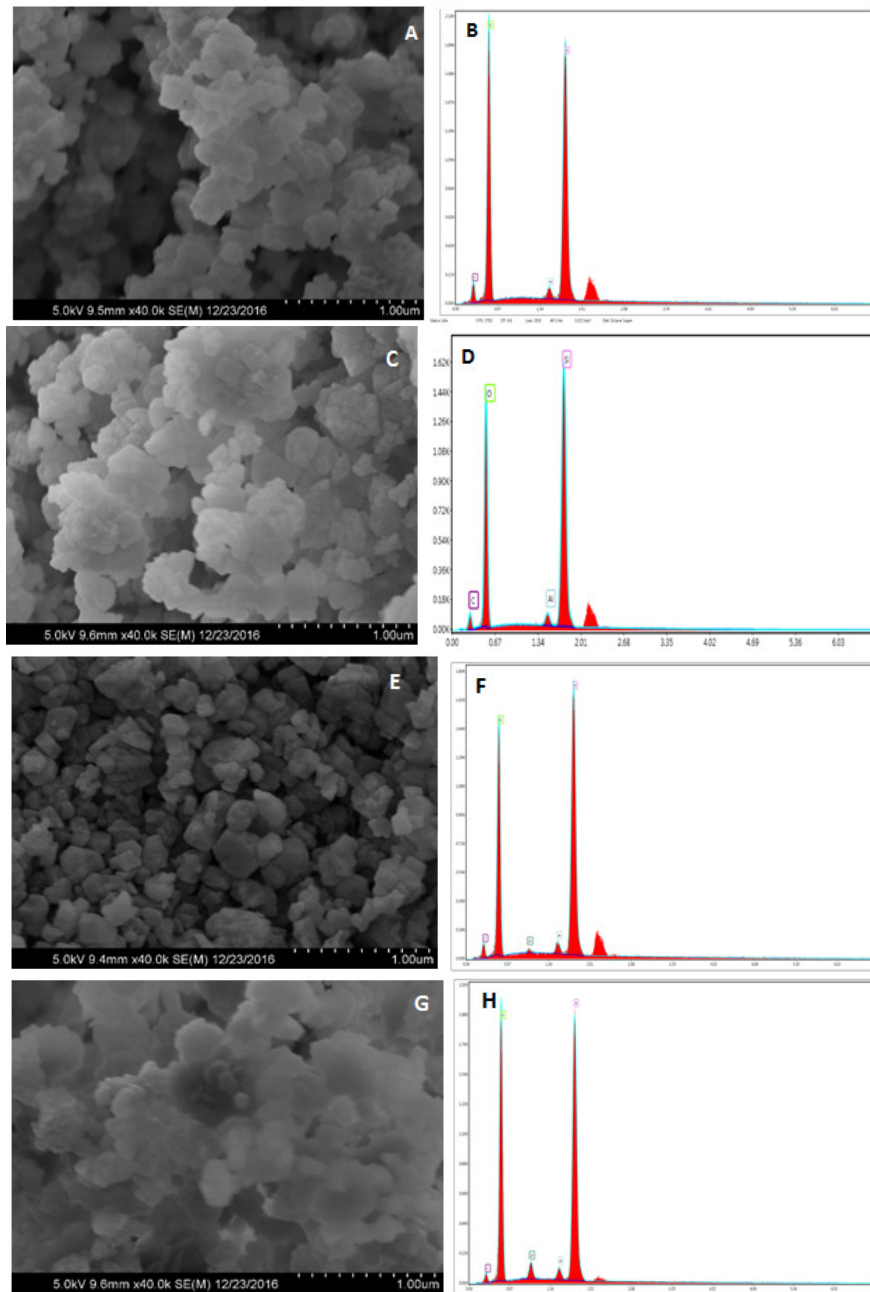


Figure 2: SEM and EDX images of images of (A/B) ZSM-5 (Si/Al=50); (C/D) 0.5 wt% Zn loading on ZSM-5; (E/F) 2 wt% Zn loading on ZSM-5; (G/H) 5 wt% Zn loading on ZSM-5

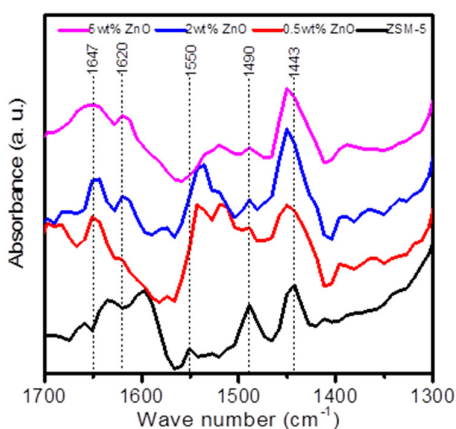


Figure 3: Pyridine IR for the catalysts

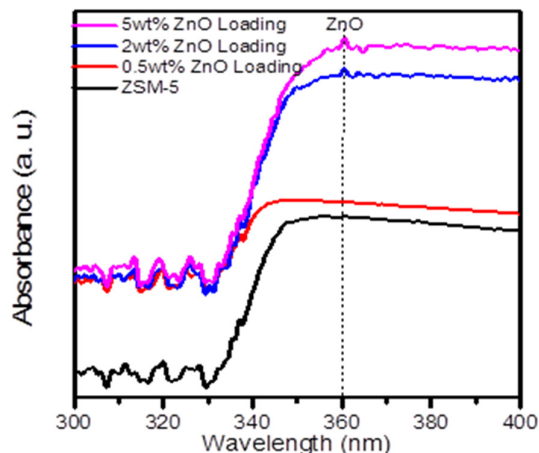


Figure 4: UV-Vis spectra of the catalysts, with ZSM-5 (50) as reference

3.2. Optimization of LPG Aromatization

Aromatization experiments using the design matrix obtained from D-optimal design of RSM (Table 2) were carried out to obtain responses from the independent experimental process variables itemized in the experimental design matrix using the quadratic model. The empirical model equation for LPG conversion relating the independent process variables and the corresponding responses is expressed in Equation (3).

$$\begin{aligned} \%LPG_{Conv} = & +111.65 + 0.87A + 44.68B + 3.93C_1 - 4.98C_2 + 1.61AB \\ & + 0.18AC_1 + 0.68AC_2 - 9.65BC_1 + 7.31BC_2 - 24.21A^2 \\ & - 40.08B^2 \end{aligned} \quad (3)$$

Where A, B, C are reaction temperature, catalyst weight, and ZnO_(.05/2)wt% loading on ZSM-5 respectively. The equation could be employed in the prediction of responses for each factor at a given level. However, it could not be used to determine the relative influence of each factor because of the scaling of the coefficients to accommodate the individual unit of each factor.

For testing the goodness of fit of the LPG conversion model, response surface quadratic model was employed because of its suitability. The coefficient of determination (R^2) was determined to be 95.61%. Adjusted and predicted R^2 were obtained as 90.78% and 56.69% respectively. However, the values are not as close as one may reasonably expect because the difference between them is >0.2 . This might be attributed to large block effects or a possible problem with the model and/or data. Model corrections, transformation of responses, outliers etc are some measures that should be considered to improve the R^2 agreement in subsequent experiments. The F-value (lack-of-fit) of 19.80 indicates that the model is significant, and shows that there is only a 0.01% chance that this value is as a result of error. As a result, the model could be used in navigating the design space. In developing a new model, it is important to carry out adequacy check to determine if the assumptions in the analysis of variance (ANOVA) are satisfied between the experimental and the simulated results. Figures 5a and 5b show the level of these agreements for the LPG conversion and aromatic selectivity and these might be ascribed to the huge block effects or problem with the model and/or data as stated earlier.

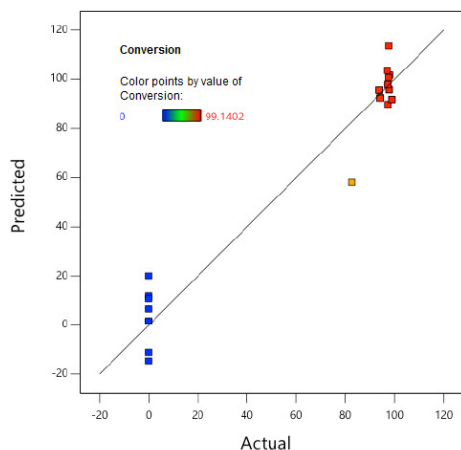


Figure 5a: Actual versus predicted extent of LPG conversion

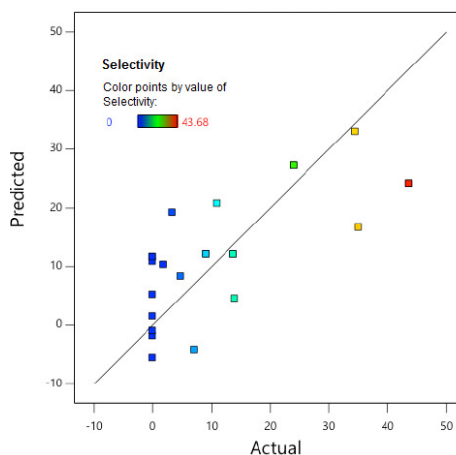


Figure 5b: Actual versus predicted extent of aromatic selectivity

The effect of interactions between experimental process variables such as reaction temperature, catalyst weight, and ZnO wt% loading on ZSM-5(50) was studied by employing the RSM 3D surface plot diagrams. Interpretation of the ANOVA (Table 4a) results for the LPG conversion indicates that the regression model is significant because of the large F-value and a small p-value.

Table 4a: ANOVA (quadratic Model) for LPG conversion

Source	Sum of Squares	df	Mean Square	F-value	p-value
Block	660.29	2	330.14		
Model	46693.47	11	4244.86	19.80	< 0.0001
A	28.57	1	28.57	0.1333	0.7227
B	34307.00	1	34307.00	160.02	< 0.0001
C	339.52	2	169.76	0.7918	0.4795
AB	30.90	1	30.90	0.1441	0.7121
AC	6.18	2	3.09	0.0144	0.9857
BC	736.26	2	368.13	1.72	0.2285
A ²	1712.27	1	1712.27	7.99	0.0180
B ²	4927.31	1	4927.31	22.98	0.0007
Residual	2143.97	10	214.40		
Lack of Fit	2143.97	5	428.79		
Pure Error	0.0000	5	0.0000		
Cor Total	49497.73	23			
Std. Dev.	14.64				
Mean	64.07				
C.V. %	22.85				
R ²	0.9561				
Adjusted R ²	0.9078				
Predicted R ²	0.5669				
Adeq Precision	11.4592				

Table 4b: ANOVA (linear model) for aromatic selectivity

Source	Sum of Squares	df	Mean Square	F-value	p-value
Block	20.22	2	10.11		
Model	2488.79	4	622.20	4.69	0.0098
A	44.33	1	44.33	0.3341	0.5708
B	1436.75	1	1436.75	10.83	0.0043
C	1251.43	2	625.71	4.72	0.0235
Residual	2255.98	17	132.70		
Lack of Fit	2255.98	12	188.00		
Pure Error	0.0000	5	0.0000		
Cor Total	4764.99	23			
Std. Dev.	11.52				
Mean	12.81				
C.V. %	94.61				
R ²	0.5245				
Adjusted R ²	0.4127				
Predicted R ²	0.0635				
Adeq Precision	6.2012				

Catalyst weight was seen as the dominant variable in the linear effect amongst others with sum of square values of 34307.00. This was followed by ZnO wt% loading on ZSM-5(50) and reaction temperature. This is attributed to the increase in the number of active sites on the catalyst surface with increase in catalyst weight and vice versa. Similarly, for the aromatic selectivity, a linear model was fitted (Table 4b). The regression model was found to be significant because of the large F and small p-values. The dominant variable was found to be the catalyst weight followed by ZnO wt% loading and reaction temperature respectively. Combined effect between catalyst weight and temperature at different ZnO wt% loading is shown in Figure 6. It was observed that temperature affects LPG conversion to a large extent. The energy requirement for the activation of butanes (the predominant component in LPG) is relatively low. Increasing the temperature enhances the decomposition of LPG to smaller molecules, thereby greatly improving the conversion. Furthermore, at higher catalyst weight, conversion is improved, which is linked to increase in the number of active sites (Scurrall, 1988).

The combined effects of reaction temperature and catalyst weight at different ZnOwt% loadings are also shown in Figures 6 (a,b,c). LPG conversion increases with temperature. At the lower design limit (520°C reaction temperature, 0.5 g catalyts weight and 5wt% ZnO loading), a conversion of 97.76% was achieved. Increasing the process conditions to upper design limit, a decrease in conversion to 94.07% was noticed. This could be attributed to the blockage of ZSM-5 (50) pores and channels by coke and volatization of zinc at higher temperatures (Seddon 1990). Optimization constraints for the three different catalysts were targeted at minimizing reaction temperature and catalyst weight while maximizing the LPG conversion and aromatic selectivity respectively. Figures 7a and 7b indicate the process requires 0.245 g catalyst weight and 5 wt% ZnO loading for optimum LPG conversion of 94.75% and aromatic selectivity of 22.38% at 520 °C.

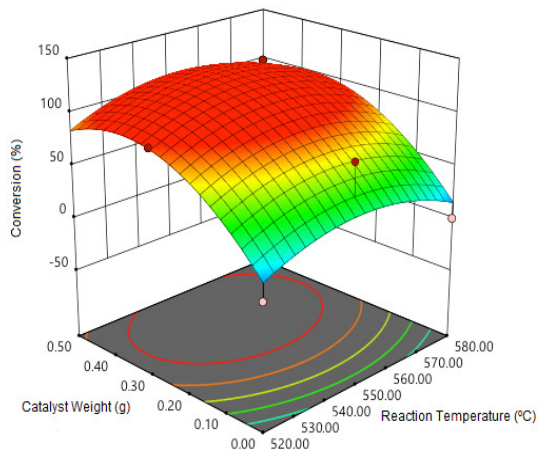


Figure 6a: Combined effects of reaction temperature, catalyst weight for 0.5 wt% ZnO loading on LPG conversion

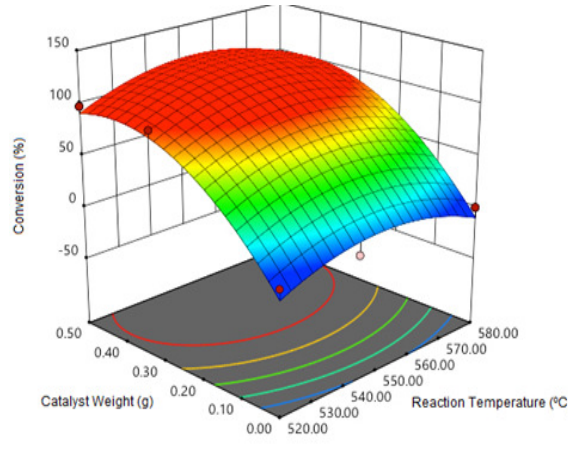


Figure 6b: Combined effects of reaction temperature, catalyst weight for 2 wt% ZnO loading on LPG conversion

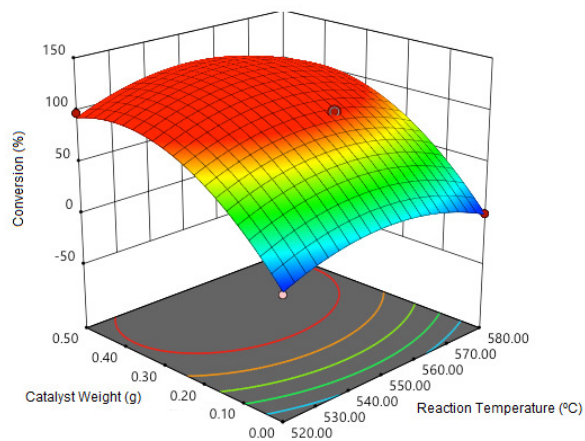


Figure 6c: Combined effects of reaction temperature, catalyst weight for 5 wt% ZnO loading on LPG conversion

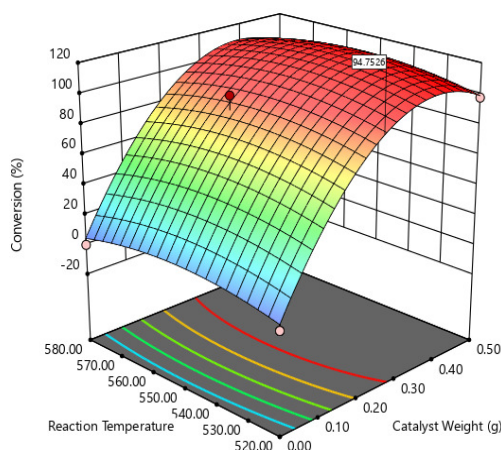


Figure 7a: Optimum condition for LPG conversion

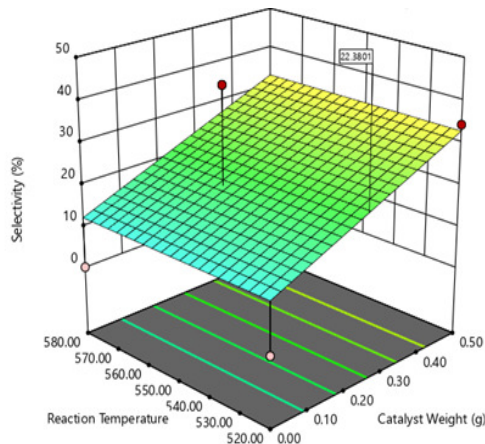


Figure 7b: Optimum condition for aromatic selectivity

It is interesting to note that the mixed feed employed in this process (LPG) makes the process more complex and affects the reaction dynamics (Seddon 1990). The presence of propane, ethane in the feed influences the product distribution and affects the conversion of the butanes. For aromatization reaction, the ease of alkane reactivity and selectivity as a function of chain length follows this order butanes>propane>ethane for the LPG feed. Also, the *i*-butanes are more reactive than *n*-butanes (Scurrall 1988). Product distributions have been found to be a function of conversion as well as the nature of the alkane feed. For a particular level of conversion, the BTEX selectivity was reported to increase with increase in conversion for the four alkanes (ethane, propane, *i*-butane and *n*-butane) and decreases with increasing conversions as the production of smaller alkanes increases (Seddon 1990). Propane and *i*-butane were reported to have comparatively high selectivity to BTEX unlike *n*-butane which has higher selectivity towards C₁-C₅ alkanes. Generally, *i*-butanes are more reactive but with lowest BTEX selectivity when compared with *n*-butanes. Propane on the other hand is associated with the lowest reactivity and the highest BTEX selectivity (Seddon 1990).

Results from experimental runs for aromatic selectivity for the three different ZnO wt% loadings is depicted in Figure 8. An improvement in the selectivity towards aromatic rather than aliphatic compounds was observed. This underscored the role of zinc in dehydrogenating and subsequent conversion of small cracked olefins to aromatics (Tshabalala and Scurrall 2015). Selectivity towards alkylated benzenes were also profound. Similarly, the three catalysts have demonstrated that aromatic formation hinders the formation of light alkenes and olefins (Niu et al., 2014).

Here also, RSM was used to determine the influence of experimental process variables on product selectivity. The ZnO/ZSM-5 catalysts studied initially exhibited high conversions close to 100% with BTEX selectivities around ~45%. A rapid decrease in activity after few hours on stream of the catalysts was linked to coke formation and zinc volatilization at the reaction temperatures (Seddon, 1990). Zinc has been reported to exhibit low vapor pressure at the conversion temperature and in the presence of strong reducing agents like hydrogen and carbon, the zinc in the catalysts elutes resulting in the decline in aromatic selectivity (Seddon, 1990). Increase in reaction temperature slightly affects product selectivity and aromatic distribution for 0.5 and 2 wt% ZnO loading. A slight decrease in BTEX selectivity was noticed while the selectivity for naphthalenes and C₉₊ aromatics rise. At reaction temperature of 520 °C, the catalysts displayed a conversion of 94.41-97.76% with BTEX selectivity of 13.99-34.45% for ZnO loadings of 0.5-5 wt%. Increasing the temperature however, results in increased conversion but selectivity suffers a decline because of dominance of LPG cracking at higher temperatures as highlighted in Figures 9 (a,b,c).

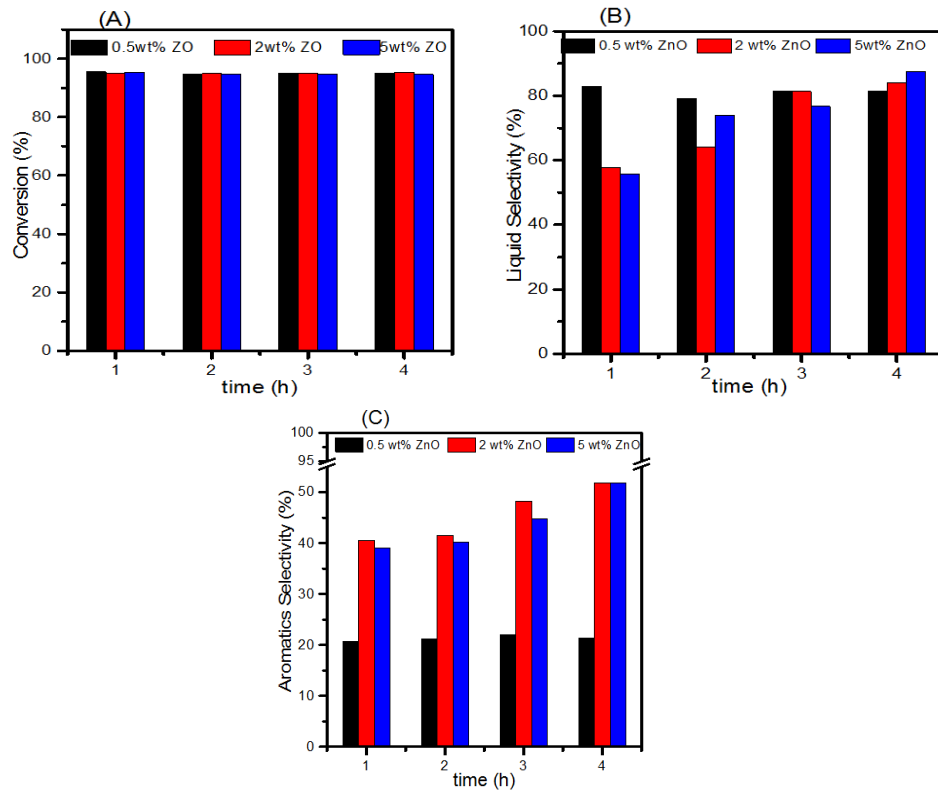


Figure 8: LPG Conversion, Liquid and Aromatic selectivity for the three different ZnO wt% loadings (a) conversion against time (b) Liquid Selectivity against time (c) Aromatics selectivity against time

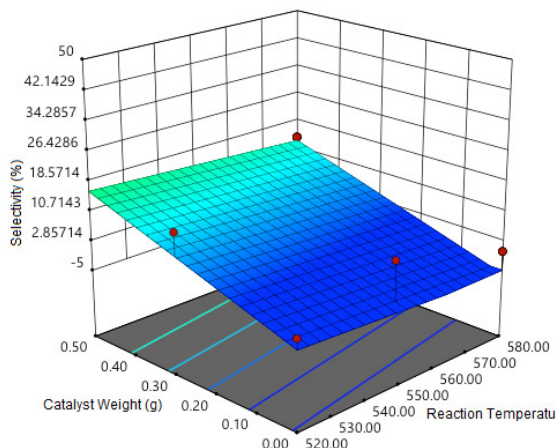


Figure 9a: Combined effects of reaction temperature, catalyst weight for 0.5 wt% ZnO loading on aromatic selectivity

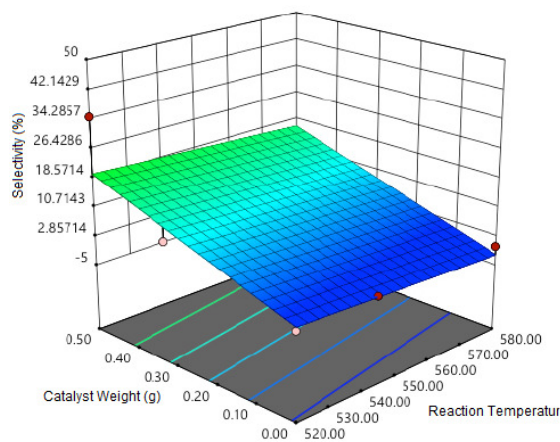


Figure 9b: Combined effects of reaction temperature, catalyst weight for 2 wt% ZnO loading on aromatic selectivity

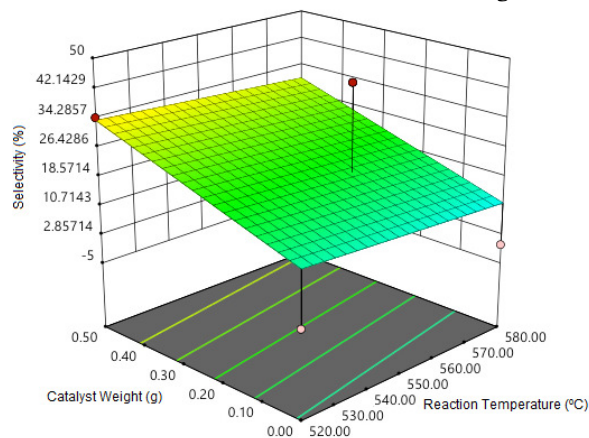


Figure 9c: Combined effects of reaction temperature, catalyst weight for 5 wt% ZnO loading on aromatic selectivity

4. CONCLUSION

Optimization of LPG aromatization process conditions over three different ZnO loaded ZSM-5 catalysts were conducted by developing a model equation. The optimization process involved these independent process variables: reaction temperature; catalyst weight; and ZnO wt% loading on ZSM-5. From the design of experiment, the interaction between these variables affected considerably the conversion of LPG over the catalysts. The combined effects of these variables on the conversion were determined based on the D-optima design of RSM. Experimental results obtained were relatively in good agreement with predictions from the model. Quadratic and linear models were employed in optimizing the conversion and selectivity respectively. An optimum LPG conversion of 94.75% could be achieved at 520 °C temperature, 0.245 g catalyst weight and 5 wt% ZnO loading.

5. ACKNOWLEDGMENT

The authors are grateful to the Petroleum Technology Development Fund (PTDF), Abuja, for the research grant provided to conduct this research.

6. CONFLICT OF INTEREST

There is no conflict of interest associated with this work.

REFERENCES

- Ai, S. N. L.H., Liu, J., He, N. and Guo, H. (2013). Catalytic conversion of n-butane over Au-Zn-modified nano-sized HZSM-5. *Chinese Journal of Catalysis*, 34 (6), pp. 1262-1266.
- Al-Khattaf, S., Ali, S.A., Aitani, A.M., Žilková, N., Kubička, D. and Čejka, J. (2014). Recent Advances in Reactions of Alkylbenzenes Over Novel Zeolites: The Effects of Zeolite Structure and Morphology. *Catalysis Reviews*, 56(4), pp. 333-402
- Caeiro, G., Carvalho, R.H., Wang, X., Lemos, M.A.N.D.A., Lemos, F., Guisnet, M. and Ramôa Ribeiro, F. (2006). Activation of C2–C4 alkanes over acid and bifunctional zeolite catalysts. *Journal of Molecular Catalysis A: Chemical*, 255(1), pp. 131-158.
- Chen, X., Dong, M., Niu, X., Wang, K., Chen, G., Fan, W., Wang, J. and Qin, Z. (2015). Influence of Zn species in HZSM-5 on ethylene aromatization. *Chinese Journal of Catalysis*, 36(6), pp. 880-888.
- Condon, J.B. (2006). Interpreting the Physisorption Isotherm, in Surface Area and Porosity Determinations by Physisorption. *Elsevier Science: Amsterdam*. pp. 55-90.
- Dragoi, B., Dumitriu, E., Guimon, C. and Auroux, A. (2009). Acidic and adsorptive properties of SBA-15 modified by aluminum incorporation. *Microporous and Mesoporous Materials*, 121(1), pp. 7-17.
- Dubey, S., Upadhyay, S.N. and Sharma, Y.C. (2016). Optimization of removal of Cr by γ -alumina nano-adsorbent using response surface methodology. *Ecological Engineering*, 97 (Supplement C), pp. 272-283.
- Frey, K., Lubango, L.M., Scurrell, M.S. and Gucci, L. (2011). Light alkane aromatization over modified Zn-ZSM-5 catalysts: characterization of the catalysts by hydrogen/deuterium isotope exchange. *Reaction Kinetics, Mechanisms and Catalysis*, 104(2), pp. 303-309.
- Fripat, N., Conanec, R., Auroux, A., Laurent, Y. and Grange, P. (1997). Influence of Nitrogen Content on Zirconophosphate Oxynitrides Acid–Base Properties. *Journal of Catalysis*, 167(2), pp. 543-549.
- Goh, E.G., Xu, X. and McCormick, P.G. (2014). Effect of particle size on the UV absorbance of zinc oxide nanoparticles. *Scripta Materialia*, 78(Supplement C), pp. 49-52.
- Gómez-Cazalilla, M., Mérida-Robles, J.M., Gurbani, A., Rodríguez-Castellón, E. and Jiménez-López, A. (2007). Characterization and acidic properties of Al-SBA-15 materials prepared by post-synthesis alumination of a low-cost ordered mesoporous silica. *Journal of Solid State Chemistry*, 180(3), pp. 1130-1140.
- Kitagawa, H., Sendoda, Y. and Ono, Y. (1986). Transformation of propane into aromatic hydrocarbons over ZSM-5 zeolites. *Journal of Catalysis*, 101(1), pp. 12-18.
- Majhi, S., Mohanty, P., Dalai, A.K. and Pant, K.K. (2013). Statistical Optimization of Process Variables for Methane Conversion over Zn-Mo/H-ZSM-5 Catalysts in the Presence of Methanol. *Energy Technology*, 1(2-3), pp. 157-165.
- Matsuoka, A., Kim, J.-B., and Inui, T. (2000). Selectivity improvement in the aromatization of C2–C5 alkanes using polyfunctional metallosilicate catalysts. *Microporous and Mesoporous Materials*, 35 (Supplement C), pp. 89-98.
- Mole, T., Anderson, J.R. and Creer, G. (1985). The reaction of propane over ZSM-5-H and ZSM-5-Zn zeolite catalysts. *Applied Catalysis*, 17(1), pp. 141-154.
- Montgomery, D.C. and Runger, G.C. (2013). *Applied Statistics and Probability for Engineers: Reg Card.*: John Wiley & Sons, Incorporated.
- Niu, X., Gao, J., Miao, Q., Dong, M., Wang, G., Fan, W., Qin, Z. and Wang, J. (2014). Influence of preparation method on the performance of Zn-containing HZSM-5 catalysts in methanol-to-aromatics. *Microporous and Mesoporous Materials*, 197(Supplement C), pp. 252-261.

- Ogunronbi, K.E., Al-Yassir, N., and Al-Khattaf, S. (2015). New insights into hierarchical metal-containing zeolites; synthesis and kinetic modelling of mesoporous gallium-containing ZSM-5 for propane aromatization. *Journal of Molecular Catalysis A: Chemical*, 406(Supplement C), pp. 1-18.
- Premanathan, M., Karthikeyan, K., Jeyasubramanian, K. and Manivannan, G. (2011). Selective toxicity of ZnO nanoparticles toward Gram-positive bacteria and cancer cells by apoptosis through lipid peroxidation. *Nanomedicine: Nanotechnology, Biology and Medicine*, 7(2), pp. 184-192.
- Seddon, D. (1990). Paraffin oligomerisation to aromatics. *Catalysis Today*, 6(3), pp. 351-372.
- Scurrall, M.S. (1988). Factors affecting the selectivity of the aromatization of light alkanes on modified ZSM-5 catalysts. *Applied Catalysis*, 41(Supplement C), pp. 89-98.
- Song, C., Liu, S., Li, X., Xie, S., Liu, Z. and Xu, L. (2014). Influence of reaction conditions on the aromatization of cofeeding n-butane with methanol over the Zn loaded ZSM-5/ZSM-11 zeolite catalyst. *Fuel Processing Technology*, 126(Supplement C), pp. 60-65.
- Tshabalala, T.E. and Scurrall, M.S., (2015), Aromatization of n-hexane over Ga, Mo and Zn modified H-ZSM-5 zeolite catalysts. *Catalysis Communications*, 72 (Supplement C), pp. 49-52.
- Viswanadham, N., Muralidhar, G. and Rao, T. P. (2004). Cracking and aromatization properties of some metal modified ZSM-5 catalysts for light alkane conversions. *Journal of Molecular Catalysis A: Chemical*, 223, pp. 269–274.
- Vosmerikova, L. N., Zaikovskii, V. I., Barbashina, Y. E. and Vosmerikov, A.V. (2014a). Deactivation of a Zn-Containing Zeolite in Ethane Aromatization. *Kinetikai Kataliz*, 55(6), pp. 748-755.
- Vosmerikova, L. N., Barbashin, Y. E. and Vosmerikov, A.V. (2014b). Catalytic aromatization of ethane on zinc-modified zeolites of various framework types. *Petroleum Chemistry*, 54(6), pp. 420–425.